A Single Amino Acid Change in the Yeast Vacuolar Metal Transporters Zrc1 and Cot1 Alters Their Substrate Specificity*

Huilan Lin, Attila Kumánovics[1], Jenifer M. Nelson, David E. Warner, Diane McVey Ward, and Jerry Kaplan[2]
From the Department of Pathology, School of Medicine, University of Utah, Salt Lake City, Utah 84132

Iron is an essential nutrient but in excess may damage cells by generating reactive oxygen species due to Fenton reaction or by substituting for other transition metals in essential proteins. The budding yeast *Saccharomyces cerevisiae* detoxifies cytosolic iron by storage in the vacuole. Deletion of *CCC1*, which encodes the vacuolar iron importer, results in high iron sensitivity due to increased cytosolic iron. We selected mutants that permitted Δ*ccc1* cells to grow under high iron conditions by UV mutagenesis. We identified a mutation (N44I) in the vacuolar zinc transporter *ZRC1* that changed the substrate specificity of the transporter from zinc to iron. *COT1*, a vacuolar zinc and cobalt transporter, is a homologue of *ZRC1* and both are members of the cation diffusion facilitator family. Mutation of the homologous amino acid (N45I) in *COT1* results in an increased ability to transport iron and decreased ability to transport cobalt. These mutations are within the second hydrophobic domain of the transporters and show the essential nature of this domain in the specificity of metal transport.

The yeast vacuole plays an important role in transition metal storage and detoxification. In conditions of metal scarcity, metals stored in the vacuole can be mobilized by specific transporters and utilized for metabolic purposes. Conversely, export of metals from cytosol to vacuole is thought to prevent metal toxicity. Yeast mutants that are unable to store iron in the vacuole, either due to a lack of vacuolar structures (1), an inability to acidify vacuoles due to mutation in the V-ATPase (2, 3), or deletion of vacuole metal transporters (4–6) show sensitivity to high concentrations of metals.

Specific transporters mediate the transport of different transition metals from cytosol to vacuole. Among the best studied of the vacuolar transition metal transporters are the zinc transporters Zrc1 and Cot1 (4, 5, 7–9). These homologous proteins, which are involved in the transport of zinc and cobalt are members of the cation diffusion facilitator (CDF)[3] family (for review

see Ref. 10). Although CDF members show differences in size, cellular localization, and substrate metals transported, they share some common features. The majority of CDF family members have six putative transmembrane domains (TMD) and a highly conserved amino acid sequence extending from TMD II to III, which is a signature motif for the family. Based on the alignment of multiple sequences, highly conserved charged residues in TMD II and V are implicated in metal binding and transport. This finding is supported by structural studies on an *Escherichia coli* CDF family member Fief (also known as YiiP), a putative Zn^{2+} and Fe^{2+} transporter (11, 12).

Transport of iron from cytosol to vacuole is mediated in yeast by Ccc1 (6) and in plants by the *CCC1* homologue VIT1 (13). These proteins define a unique family that appears to be restricted to fungi and plants. Little is known of the mechanism of transport, although it is clear that *CCC1* is regulated by iron at transcriptional and post-transcriptional levels (14, 15). Deletion of *CCC1* results in poor growth in high iron medium indicating that increased cytosolic iron may be toxic (6). The mechanism(s) leading to high iron toxicity is unknown. High iron toxicity occurs in cells deleted for *CCC1* even in the absence of respiratory capacity (*e.g.* rho° cells) or anaerobically (16). These results call into question the assumption that high iron toxicity is due to the generation of iron-mediated reactive oxygen radicals. In an effort to define the mechanism of iron toxicity we initiated a genetic screen in which we identified mutant strains of Δ*ccc1* that grew on high iron. Herein, we identify a missense mutation in the vacuolar zinc transporter Zrc1, which completely changes the substrate specificity of this transporter from Zn^{2+} to Fe^{2+}. We show that a similar amino acid change in the homologous Cot1, a Co^{2+} and Zn^{2+} transporter, also results in a change in metal specificity.

EXPERIMENTAL PROCEDURES

Yeast Strains—The following yeast strains (W303 background) were used: DY150 (*Mat**a** ade2-1 his3-11 leu2-3,112 trp1-1 ura3-52 can1-100(oc)*) and DY1457 (*Matα ade6 his3-11 leu2-3,112 trp1-1 ura3-52 can1-100(oc)*). Deletions of *CCC1* and *ZRC1* were generated by double fusion polymerase chain reaction using the *HIS3* gene as a selectable marker (17). Primers for disruption of *CCC1* were described (6). Primers for disruption of *ZRC1* were Pri20−78 (5′-TCT CTT TTG ACC TTA GAC ACG-3′), Pri20−79 (5′-GTC GTG ACT GGG AAA ACC

[3] The abbreviations used are: CDF, cation diffusion facilitator family; BPS, bathophenanthroline disulfonate; CM, complete medium; ICP, inductively coupled plasma-optical emission spectrometer; TMD, transmembrane domain; YPD, yeast extract peptone dextrose medium.

CTG GCG ATC GCT GCC ATG ATC GTG GAA-3′), Pri20–80 (TCC TGT GTG AAA TTG TTA TCC GCT GCT GAT CAG ATT CAA AGA GAG-3′), and Pri20–81 (GCA GTT TAC AGC GTC ATC TAC-3′). The *COT1* gene was disrupted using *URA3* as described (4). Strains with a *FET3-lacZ* reporter integrated at the *HO* locus were constructed as described (18). Wild type BY4743 (*Mat* **a**/**α** *his3Δ1/his3Δ1 leu2Δ0/leu2Δ0 lys2Δ0/+ met15Δ0/+ ura3Δ0/ura3Δ0*), Δ*cot1*::*KanMX* and Δ*pmr1*::*KanMX* strains in the BY4743 background were obtained from Research Genetics.

Growth Media—Yeast strains were grown in YPD medium (1% yeast extract, 2% peptone, 2% dextrose) or in CM medium (0.67% yeast nitrogen base without amino acids, 2% dextrose, and 0.13% amino acid drop-out mixture). Low iron growth medium was made by adding 40 μM bathophenanthroline disulfonate (BPS), an iron chelator, to CM and then the addition of specified amounts of $FeSO_4$. To make high iron plates, ferrous ammonium sulfate (250 mM stock in water) was added into media to give the indicated iron concentrations. $FeSO_4$ (50 mM stock in 0.1 M HCl) was used in liquid culture as indicated together with a final concentration of 1 mM ascorbic acid.

Isolation of Mutants—DY150 Δ*ccc1* or DY1457 Δ*ccc1* cells were plated on CM agar plates at a density of 500 cells/plate and exposed to UV light to give a 50% survival. Mutagenized cells were grown for 2 days and then replicated to CM plates containing 5 mM ferrous ammonium sulfate. Cells were grown for another 3 days. Colonies able to grow on high iron were selected for further study.

Identification of ZRC1(N44I)—The mutated gene in dominant mutant R1 was identified by constructing a library from the R1 genomic DNA using standard protocols (19). Briefly, Sau3A partially digested genomic DNA was fractionated on a 10–40% sucrose gradient, and centrifuged at 25,000 × *g* for 22 h. The 8–10-kb genomic fraction was ligated to pRS416-zero, a centromeric plasmid, digested with BamHI and dephosphorylated with calf intestinal phosphatase (New England Bio-Labs). Ligation products were transformed into Electromax™ DH10B™ *E. coli* (Invitrogen) (20). Plasmids were extracted from transformed bacteria and pooled. The pooled library was transformed into Δ*ccc1* cells and plasmids that conferred resistance to high iron (3 mM) were recovered. The genomic fragments in these plasmids were identified by sequencing.

Plasmids Construction and Site-directed Mutagenesis—*ZRC1(N44I)* was subcloned from the genomic library using KpnI and BglII and inserted into pRS416 (a yeast centromeric vector), which had been digested with BamHI and KpnI. Wild type *ZRC1* with its own promoter and 3′ end was generated using PCR from genomic DNA using pri54 (5′-GAT ATG AAA GTA GTT GCA TT-3′) and pri60 (5′-TTG GTA CAG GAG GGA ACA AG-3′). The PCR fragment was digested with BglII and KpnI and inserted into pRS416 digested with BamHI and KpnI. To introduce the N44I mutation into wild type *ZRC1*, pri64 (5′-GGC CTT GAT TGC CGA TTC ATT TCA CAT GTT GAT TGA TAT CAT CTC TCT TTT AGT GGC-3′) and pri65 (5′-GCC ACT AAA AGA GAG ATG ATA TCA ATC AAC ATG TGA AAT GAA TCG GCA ATC AAG GCC-3′) were used. To introduce the D45A mutation into wild type *ZRC1*, pri102 (5′-CAC ATG TTG AAT GCT ATC ATC TCT

CTT TTA GTG GCA C-3′) and pri103 (5′-GTG CCA CTA AAA GAG AGA TGA TAG CAT TCA ACA TGT G-3′) were used. *COT1*/YEp352 was obtained from Dr. Douglas S. Conklin (4). To introduce N45I into wild type *COT1*, pri66 (5′-CGC GGA CTC ATT CCA TAT GCT AAT CGA TAT AAT TTC TCT TGT GG-3′) and pri67 (5′-CCA CAA GAG AAA TTA TAT CGA TTA GCA TAT GGA ATG AGT CCG CG-3′) were used. Site-directed mutagenesis was performed with the QuikChange site-directed mutagenesis kit from Stratagene according to the manufacturer's instructions. *ZRC1* and *ZRC1(N44I)* were digested with KpnI and XbaI and inserted into a yeast episomal vector pTF62 (*LEU2* marker). To generate His$_6$-tagged versions of *CCC1*, *ZRC1*, and *ZRC1(N44I)* under the control of the galactose inducible promoter (*GAL1*) the following primers were used: *CCC1*, pri78 (5′-CGC GGA TCC ATG TCC ATT GTA GCA CTA AAG-3′) and pri79 (5′-CCG GAA TTC ACC CAG TAA CTT AAC AAA GAA-3′), for *ZRC1* and *ZRC1(N44I)*, pri80 (5′-GGG CGA AGA TCT ATG ATC ACC GGT AAA GAA TTG-3′) and pri81 (5′-CCG GAA TTC CAG GCA ATT GGA AGT ATT GCA-3′). DNA was amplified by PCR to generate each open reading frame without the stop codon. The amplified products were inserted into BamHI- and EcoRI-digested pYES2/CT (Invitrogen).

Metal Analysis—For whole cell metal analysis, 20 OD cells (about 2×10^8 cells) at log phase were collected, washed three times with 50 mM Tris-Cl (pH 6.5), 10 mM EDTA and once with deionized water. Vacuoles were prepared using Ficoll gradients as described previously (6). Samples were digested in 200 μl of nitric acid at 80 °C for 1 h, then diluted to 1.0 ml with deionized water. Metals were analyzed in a Perkin-Elmer Inductively Coupled Plasma-Optical Emission Spectrometer (ICP) and calculated using a standard curve generated from mixed metal standards.

Western Blot, β-Galactosidase Activity, and Protein Concentration Assay—Cells were disrupted with glass beads in the presence of protease inhibitors (1.0 mM phenylmethylsulfonyl fluoride, 1.0 μM pepstatin A, and 1.0 μM leupeptin) (Sigma). Samples (20 μg) were run on a 12% SDS-PAGE, transferred to nitrocellulose, and probed with rabbit anti-His$_6$ tag (1:2000 Abcam) or mouse anti-Vma1 antibody (1:4000, Molecular Probes), followed by peroxidase-conjugated goat anti-rabbit or goat anti-mouse antibody (1:10,000, Jackson Immuno-Research). Membranes were developed using chemiluminescence reagents (PerkinElmer Life Sciences). The reporter constructs *FET3-lacZ* and *CCC1-lacZ* were described previously (15, 18). β-Galactosidase activity was performed in 96-well plates using *ortho*-nitrophenyl-β-galactoside as a substrate. The generation of *ortho*-nitrophenol was monitored at 420 nm and the data are presented as nanomole/min/mg of protein (18). Protein concentration was determined by the bicinchoninic acid method (Pierce) using bovine serum albumin as standard.

RESULTS

Identification of Yeast Mutants Resistant to High Iron—Deletion of *CCC1* results in sensitivity to high iron (6, 15). We took advantage of this phenotype to identify UV-induced mutants of Δ*ccc1* cells that were capable of growth on high iron medium.
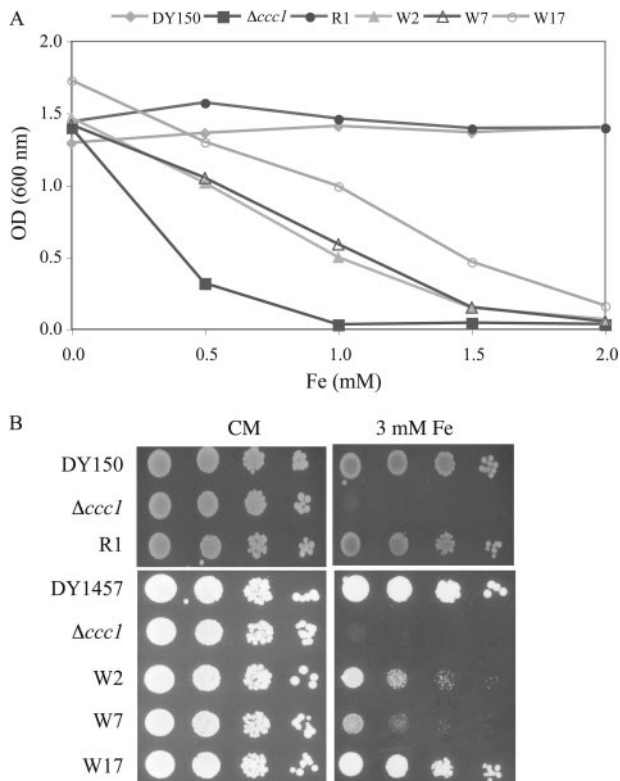
FIGURE 1. **Δ*ccc1* cells mutagenized by UV are resistant to high iron.** *A*, DY150 (wild type), Δ*ccc1*, and the Δ*ccc1* mutants isolated after UV mutagenesis. R1, W2, W7, and W17 were grown to log phase in CM medium and then inoculated at a starting OD of 0.005 into CM medium with ferrous ammonium sulfate at the indicated concentrations. Cells were incubated at 30 °C overnight and the cell density was measured by absorbance at 600 nm. The experiment was performed multiple times and a representative experiment is presented. *B*, DY150 (wild type), DY150 Δ*ccc1*, R1 mutant, DY1457 (wild type), DY1457 Δ*ccc1*, and W2, W7, and W17 mutants were grown to log phase in CM medium and 10^4, 10^3, 10^2, and 10^1 cells spotted onto CM plates or CM plates with 3 mM ferrous ammonium sulfate. Plates were incubated at 30 °C for 2 days. The color difference of the colonies is due to different *ade* mutations (see "Experimental Procedures" for genotype).

We screened 12,400 colonies and identified 15 mutants that would survive on high iron medium. The mutants were backcrossed to the parental strain (Δ*ccc1*) to determine whether they were single gene defects and whether the mutants were dominant or recessive. Seven of the mutants were single gene recessive mutations that fell into two complementation groups. Eight of the mutants were dominant. The mutants were characterized as having different sensitivity to high iron, as shown by liquid (Fig. 1*A*) and plate growth assays (Fig. 1*B*).

There are several potential mechanisms that might lead to high iron-resistant growth: decreased iron uptake, increased iron export, increased iron storage, or increased antioxidant defenses. To determine whether the mutant strains had decreased iron acquisition, cells were grown in CM medium overnight and cellular iron levels were measured by ICP. Mutants W2 and W7 accumulate less iron than control Δ*ccc1* cells. R1 and W17 accumulated more iron than the parental Δ*ccc1* strain (Fig. 2*A*). If resistance to high iron was due to increased iron export from cells, then the mutant strains might not grow on low iron. This situation was observed for a mutant *PDR1* in which high iron resistance was correlated with low iron sensitivity (21). The Δ*ccc1* mutant strains were able to

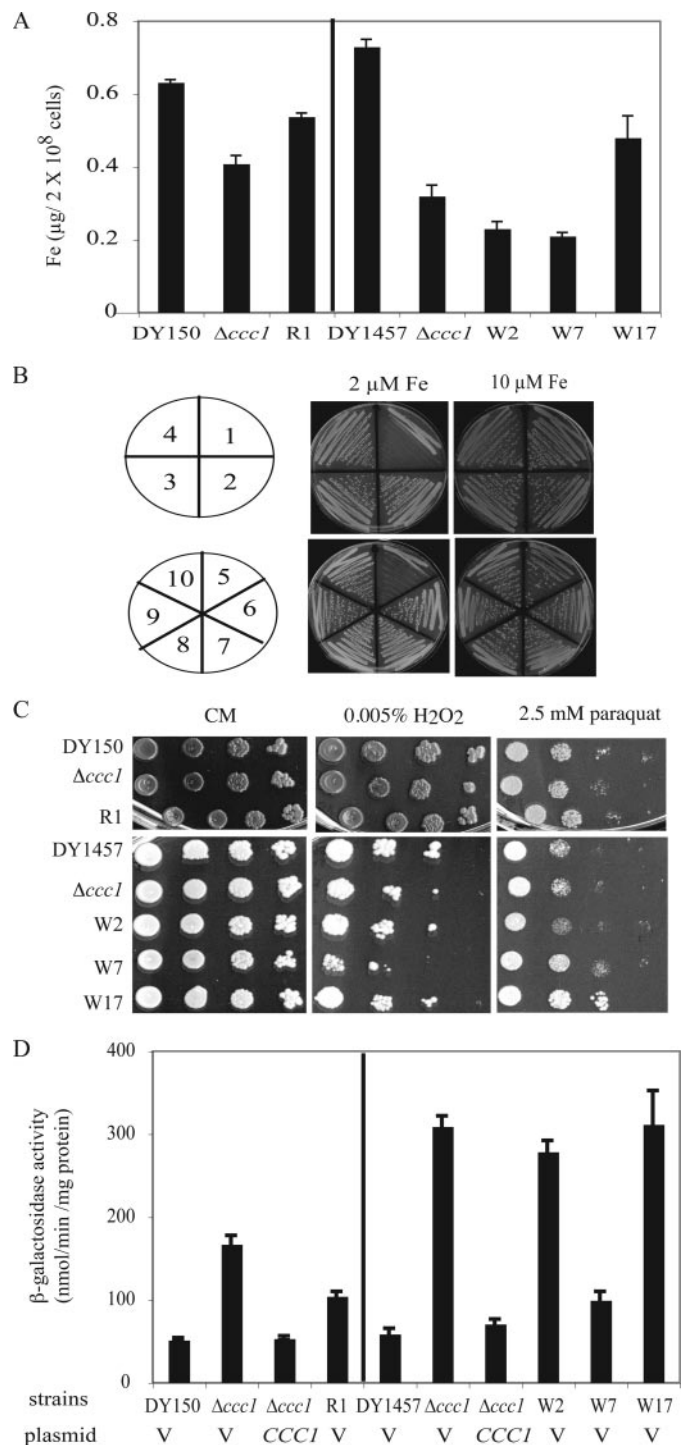FIGURE 2. **Characteristics of high iron-resistant Δ*ccc1* mutants.** *A*, DY150, DY150 Δ*ccc1*, R1 mutant, DY1457, DY1457 Δ*ccc1* and W2, W7, and W17 mutants were grown in CM medium overnight. 20 OD cells (2×10^8) were collected, washed, and digested in nitric acid and iron contents were determined by ICP. *B*, strains were streaked onto CM plates containing 40 μM BPS with 2 and 10 μM $FeSO_4$ added back. Plates were incubated at 30 °C for 2 days. *1*, Δ*fet3*; *2*, DY150; *3*, DY150Δ*ccc1*; *4*, R1 mutant; *5*, Δ*fet3*; *6*, DY1457; *7*, DY1457Δ*ccc1*; *8*, W2; *9*, W7; *10*, W17. *C*, cells as in *A* were grown in CM medium, spotted onto CM or CM with 0.005% H_2O_2 or 2.5 mM paraquat. Plates were incubated at 30 °C for 2 days. *D*, cells as in *A* were transformed with a reporter construct *CCC1-lacZ* and either a control vector (*V*) or a low copy *CCC1* plasmid. The cells were grown in CM-Leu-Ura medium to log phase, harvested, and β-galactosidase activity determined. The data were normalized for protein concentration and *error bars* represent S.D. from three experiments.

grow on iron-limited medium, which requires a functional iron transport system (Fig. 2*B*). These results suggest that the resistance to high iron cannot be explained only by decreased iron acquisition or increased iron export. If iron toxicity was due to increased oxidative damage resulting from Fenton chemistry, then increased antioxidant defenses might reduce such damage. To test this possibility we examined the ability of mutant cells to resist the effect of the oxidants H_2O_2 and paraquat. One mutant (W17) showed a slight increase in paraquat resistance, but in general the mutants were as sensitive to oxidants as the parental strains (Fig. 2*C*).

We tested the possibility that the mutants were able to store or sequester cytosolic iron by measuring the expression of an iron-responsive reporter. Transcription of *CCC1* or a *CCC1-lacZ* reporter construct is increased by iron through activation of the transcription factor Yap5 (15). Wild type, Δ*ccc1*, and Δ*ccc1* mutants were transformed with a *CCC1-lacZ* construct and the effect of iron on induction of β-galactosidase activity was determined. Compared with wild type cells, Δ*ccc1* cells showed a higher expression of *CCC1-lacZ*, indicating the presence of increased cytosolic iron. This induction of *CCC1-lacZ* was repressed when the *CCC1* gene was introduced back to Δ*ccc1* cells (Fig. 2*D*). Mutants W2 and W17 showed similar amounts of *CCC1-lacZ* activity compared with the parental Δ*ccc1* strain. R1 and W7, however, showed lower levels of β-galactosidase compared with the parental strains. The R1 mutant was the most resistant to growth inhibition by high iron (*cf.* Fig. 1*A*). Mutant R1 had a slight increase in cellular iron compared with Δ*ccc1* but less cytosolic iron as indicated by the *CCC1-lacZ* reporter assay. This implies that the resistance to high iron growth might be due to its ability to sequester cytosolic iron. Taken together these results showed that different mechanisms may contribute to high iron resistance in mutant strains.

The High Iron Resistance of Mutant R1 Is Caused by a Mutation in ZRC1—To identify the gene responsible for the high iron resistance of R1 a low copy genomic library was generated from R1 cells. The library was transformed into the Δ*ccc1* cells and transformants able to grow on high iron were identified. Plasmids conferring resistance to high iron were isolated and the genes on the insert were identified. Several plasmids containing overlapping segments of chromosome XIII were isolated. *ZRC1*, a gene that encodes a vacuolar zinc transporter (5, 22), was identified as a common gene on all rescued plasmids. Subcloning of the insert showed that the R1-specific *ZRC1* plasmid conferred iron resistance when transformed into Δ*ccc1* cells (data not shown). Sequence analysis of R1-*ZRC1* revealed a mutation at position 131 of the coding sequence that altered an adenine to thymidine, which resulted in the substitution of isoleucine for asparagine at amino acid position 44 (referred to henceforth as *ZRC1(N44I)*). To confirm that this single amino acid change was responsible for high iron resistance, the asparagine at position 44 of the wild type Zrc1 was changed to an isoleucine by site-directed mutagenesis. When transformed into Δ*ccc1* cells, *ZRC1(N44I)* was able to confer high iron resistance to Δ*ccc1* cells (Fig. 3*A*).

Zrc1 was identified initially as a high copy suppressor of zinc-sensitive growth (5) and deletion of *ZRC1* increases zinc sensitivity (7). Cells with a deletion in *ZRC1* showed zinc-sensitive
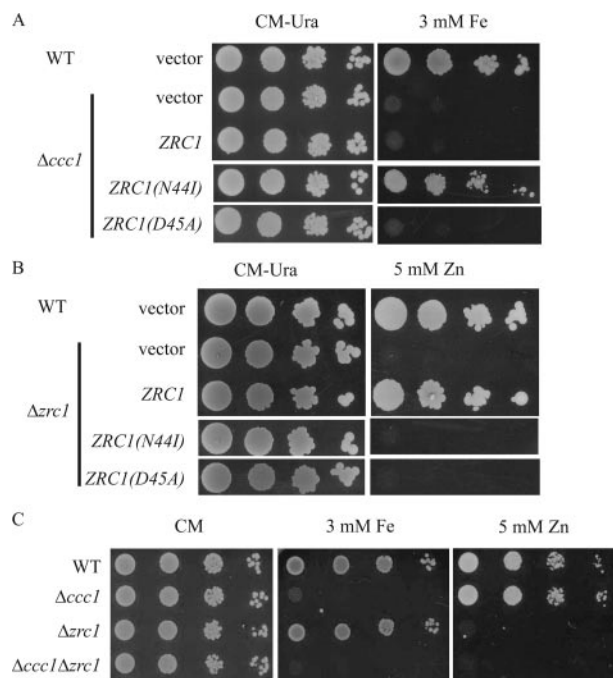

FIGURE 3. **ZRC1(N44I) confers resistance to high iron.** *A*, wild type (*WT*) cells transformed with empty vector and Δ*ccc1* transformed with empty vector, *ZRC1*, *ZRC1(N44I)*, or *ZRC1(D45A)* were spotted onto CM-Ura plates with or without 3 mM ferrous ammonium sulfate. Plates were incubated at 30 °C for 2 days. *B*, wild type and Δ*zrc1* cells transformed with empty vector *ZRC1*, *ZRC1(N44I)*, or *ZRC1(D45A)* were spotted on CM-Ura plates with or without 5 mM ZnSO₄. Plates were incubated at 30 °C for 2 days. *C*, WT, Δ*ccc1*, Δ*zrc1*, or Δ*ccc1*Δ*zrc1* cells were spotted on CM with or without 3 mM ferrous ammonium sulfate or 5 mM ZnSO₄. Plates were incubated at 30 °C for 2 days.

growth that was suppressed by expression of plasmid containing *ZRC1* but not by a plasmid containing *ZRC1(N44I)* (Fig. 3*B*). This result demonstrates that Zrc1(N44I) has lost its intrinsic zinc transport activity, and may explain why the R1 mutant is sensitive to high zinc concentration (data not shown).

It is possible that a loss of function of *ZRC1* protects Δ*ccc1* from high iron toxicity by altering zinc homeostasis and modulating the entire yeast transcriptome. To test this we generated a mutant *ZRC1* based on the sequence alignment of Zrc1 with the *E. coli* FieF, another member of the cation diffusion facilitator family (23). The crystal structure of FieF suggests that Asp[49] is involved in binding the zinc substrate. The homologous residue in Zrc1 is Asp[45] and site-specific mutagenesis of *ZRC1(D45A)* resulted in an expressed protein that was unable able to protect Δ*zrc1* cells from high zinc toxicity (Fig. 3*B*). This construct was unable to permit Δ*ccc1* cells to grow on high iron medium (Fig. 3*A*). Furthermore, deletion of *ZRC1* in Δ*ccc1* cells did not protect Δ*ccc1* from high concentrations of iron (Fig. 3*C*). Together, these data suggest that loss of zinc transport activity is not sufficient to protect Δ*ccc1* from high iron toxicity and also explains why mutant R1 shows dominant characteristics.

Zrc1(N44I) Increased Vacuolar Iron—Because Zrc1 localizes to the vacuolar membrane (9), it is possible that Zrc1(N44I) transports iron into the vacuole, which would decrease cytosolic iron. We tested this possibility by assaying the expression of a *FET3-lacZ* reporter. This reporter construct is regulated by the low iron sensing transcription factor Aft1 (24). Overexpres-
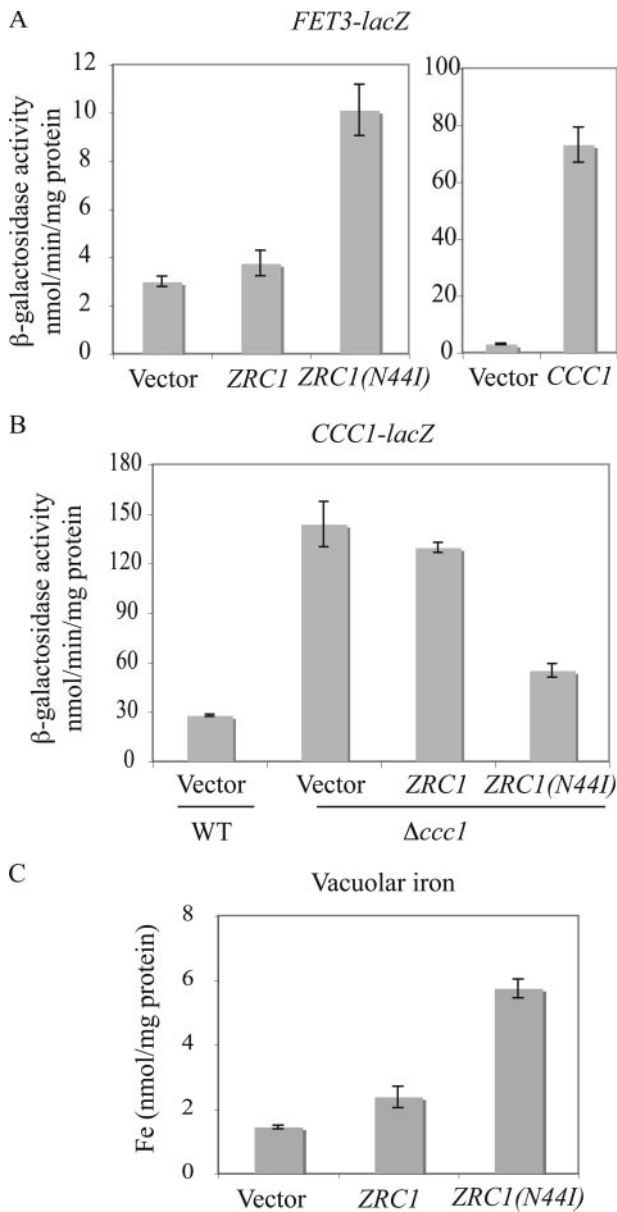
FIGURE 4. ***ZRC1(N44I)* alters cytosolic iron by transporting iron into the vacuole.** *A*, wild type (*WT*) cells with integrated *FET3-lacZ* were transformed with empty vector, *ZRC1*, *ZRC1(N44I)*, or *CCC1* under their own promoters. Cells were grown to log phase and β-galactosidase activity determined. *B*, WT cells with empty vector, Δ*ccc1* cells with empty vector, *ZRC1*, or *ZRC1(N44I)* were transformed with a *CCC1-lacZ* reporter construct. Cells were grown in CM medium to log phase and β-galactosidase activity determined. *C*, Δ*ccc1* cells transformed with a high copy empty vector, *ZRC1*, or *ZRC1(N44I)* under the *ZRC1* promoter were grown in CM medium with 50 μM FeSO$_4$ overnight. Vacuoles were isolated and iron content was determined by ICP. All data were normalized for protein concentrations and *error bars* represent S.D. from three experiments.

sion of *CCC*1, by transporting iron into vacuoles, leads to lower cytosolic iron inducing the expression of a *FET3-lacZ* reporter (6) (Fig. 4*A*). Expression of *ZRC1(N44I)* was also able to induce *FET3-lacZ* activity compared with cells transformed with either a vector or wild type *ZRC1*. Conversely, expression of *ZRC1(N44I)* but not wild type *ZRC1* was able to reduce the activity of a *CCC1-lacZ* reporter construct (Fig. 4*B*). These results confirm that expression of *ZRC1(N44I)* lowers cytosolic iron. To prove that Zrc1(N44I) transports iron into vacuoles,

iron was measured in vacuoles isolated from Δ*ccc1* cells transformed with empty vector or plasmids expressing *ZRC1* or *ZRC1(N44I)*. Overexpression of wild type *ZRC1* showed a slight increase in vacuolar iron relative to vector-transformed cells (Fig. 4*C*). Overexpression of *ZRC1(N44I)*, however, resulted in a 3–4-fold increase in vacuolar iron. Together, these results show that *ZRC1(N44I)* is a gain of function allele that can confer iron-resistant growth by exporting iron from cytosol to vacuole.

These data show that Zrc1(N44I) can transport iron but it is hard to compare the intrinsic iron transport activity of Zrc1(N44I) with that of Ccc1, as expression of each transporter is regulated differently. *CCC1* transcription and mRNA stability are increased by iron, whereas *ZRC1* (and by implication *ZRC1(N44I)*) shows increased transcription due to low zinc (7). To determine the intrinsic iron transport activity of Ccc1, Zrc1, and Zrc1(N44I), each was cloned into a *GAL1*-regulated vector. We placed a His$_6$ epitope at the carboxyl terminus of each gene, which permitted us to determine protein levels. *GAL1* regulated *CCC1-HIS$_6$* and *ZRC1(N44I)-HIS$_6$* were able to suppress the high iron growth defect of Δ*ccc1* cells, whereas as a *GAL1* regulated *ZRC1-HIS$_6$* was not (Fig. 5*A*). Under similar growth conditions, Zrc1-HIS$_6$ and Zrc1(N44I)-HIS$_6$ were expressed to higher levels than Ccc1-HIS$_6$ (Fig. 5*B*). Measurement of iron transport activity based on *FET3-lacZ* expression showed that Zrc1-HIS$_6$ had no measurable iron transport activity, whereas both Zrc1(N44I)-HIS$_6$ or Ccc1-HIS$_6$ induced expression of *FET3-lacZ* (Fig. 5*C*). Based on the expression levels of the proteins Zrc1(N44I)-HIS$_6$ has ~10–15% of the iron transport activity of Ccc1-HIS$_6$. Δ*ccc1* cells transformed with empty vector or galactose-regulated constructs were grown in galactose medium with 100 μM FeSO$_4$. Vacuoles were isolated and iron content determined. Overexpression of *CCC1-HIS$_6$* and *ZRC1(N44I)-HIS$_6$*, but not *ZRC1-HIS$_6$* increased vacuolar iron compared with vector-transformed control cells (Fig. 5*D*). There was more iron in Ccc1-HIS$_6$ vacuoles than in Zrc1(N44I)-HIS$_6$ vacuoles, again indicating that Ccc1 was more efficient in transporting iron into vacuoles.

It might be possible that iron is not transported into the vacuole but rather the iron is tightly bound to the cytosolic facing surface of Zrc1(N44I). The difference in vacuolar iron between Δ*ccc1* cells overexpressing *ZRC1(N44I)* and control cells (empty vector) was about 10–12 nmol/mg of vacuolar protein. The crystal structure of the *E. coli* CDF family member FieF suggests that it has 4 Zn binding sites (11). Assuming one molecule of Zrc1(N44I) binds 4 atoms of iron, then based on the molecular mass of Zrc1 (48,344 daltons), would require ~0.12–0.15 mg of Zrc1 protein/mg of vacuole protein to bind the measured iron. This means that Zrc1(N44I) would have to constitute 12–15% of vacuolar proteins. To test this prediction we grew Δ*ccc1* cells, transformed with either a control vector or *GAL*-regulated *ZRC1(N44I)* in galactose medium overnight and then in galactose medium containing 100 μM FeSO$_4$ for 4 h. Cells were harvested, vacuolar iron determined, and vacuolar proteins applied to SDS-PAGE and the gel analyzed by Western blot and silver stain. Vacuoles isolated from control cells only showed a slight increase in iron over the time course of the experiment, probably due to endocytosis of iron from the cul-
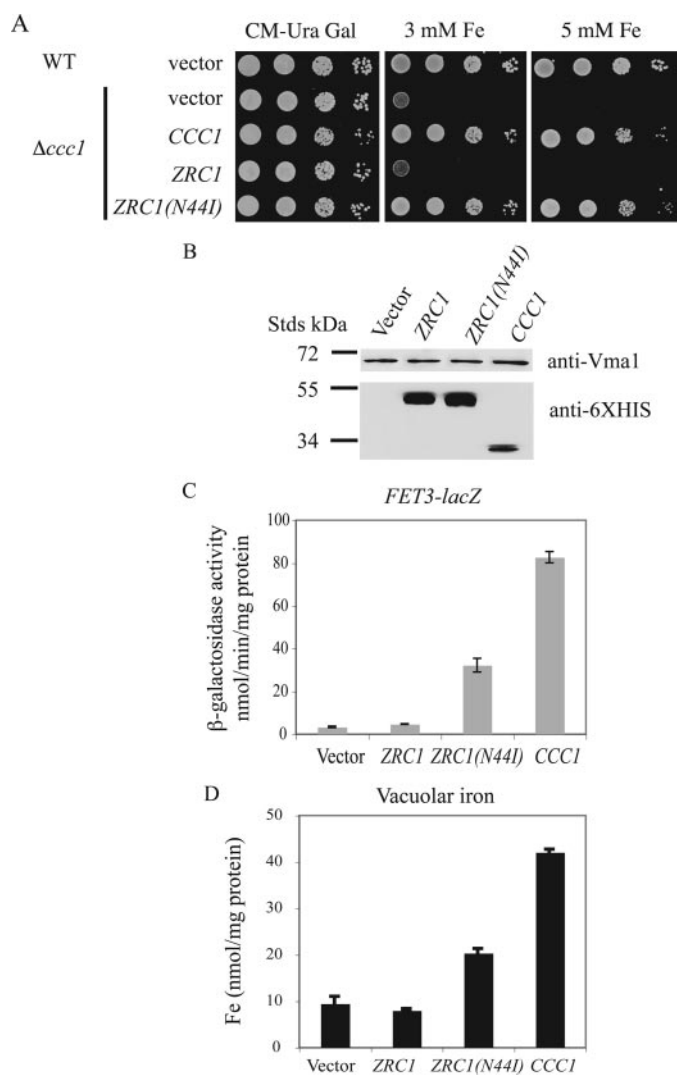
FIGURE 5. **Iron transport efficiency of Zrc1(N44I).** *A*, wild type (*WT*) cells transformed with empty vector (pYES2 *GAL1* promoter), Δ*ccc1* cells transformed with pYES2, *ZRC1*, *ZRC1(N44I)*, or *CCC1* tagged with His$_6$ at the carboxyl terminus were grown in CM with 2% raffinose at 30 °C overnight. Cells were washed and spotted onto CM-Ura medium containing 2% galactose with or without 3 or 5 mM ferrous ammonium sulfate. Plates were incubated at 30 °C for 3 days. *B*, Δ*ccc1* cells as in *A* were grown in CM medium with 2% raffinose then inoculated into CM medium with 2% galactose for 12 h. Cells were harvested, disrupted by glass beads, and protein levels measured by Western blot using a rabbit anti-His$_6$ antibody or a mouse anti-Vma1 antibody followed by peroxidase-conjugated goat anti-rabbit IgG or goat anti-mouse IgG. The vacuolar protein Vma1 was used as a loading control. *C*, Δ*ccc1* cells with an integrated *FET3-lacZ* at the *HO* locus were transformed with empty vector pYES2, *ZRC1*, *ZRC1(N44I)*, or *CCC1* as in *A*. Cells were grown in CM medium with 2% raffinose and inoculated into CM with 2% galactose for 12 h. Cells were harvested and β-galactosidase activity determined. The data are normalized for protein concentrations and *error bars* represent S.D. from three experiments. *D*, cells as in *A* were grown in CM-Ura medium containing 2% galactose with 100 μM FeSO$_4$ and 1 mM ascorbate overnight. Vacuoles were isolated and iron content was determined by ICP. All data were normalized for protein concentrations and *error bars* represent S.D. from three experiments.

FIGURE 6. **Measurement of vacuolar iron content and Zrc1(N44I) protein abundance.** *A*, Δ*ccc1* cells were transformed with a control vector (pYES2) or a *ZRC1(N44I)-HIS$_6$* containing plasmid. Cells were grown in galactose CM overnight and then incubated in the same medium containing 100 μM FeSO$_4$. Vacuoles were isolated from control and *ZRC1(N44I)* expressing cells at time 0 and 4 h after incubation in iron-rich medium. The iron content of isolated vacuoles was determined by ICP and the data normalized to protein content. *B*, isolated vacuoles were solubilized and analyzed by SDS-PAGE and Western blot using a rabbit anti-His$_6$ antibody or a mouse anti-carboxypeptidase Y antibody followed by peroxidase-conjugated goat anti-rabbit IgG or goat anti-mouse IgG. *C*, the same samples as in *B* were also analyzed by silver staining. The *arrow* represents the predicted mass of Zrc1(N44I)-HIS$_6$.

ture media. Vacuoles isolated from Zrc1(N44I) showed a much greater increase in vacuolar iron (Fig. 6*A*). Western blot showed that during this time course, the Zrc1(N44I)-HIS$_6$ protein was expressed and remained constant (Fig. 6*B*). Silver staining of vacuolar proteins from both control and Zrc1(N44I)-HIS$_6$ expressing cells had a similar protein distribution in which the
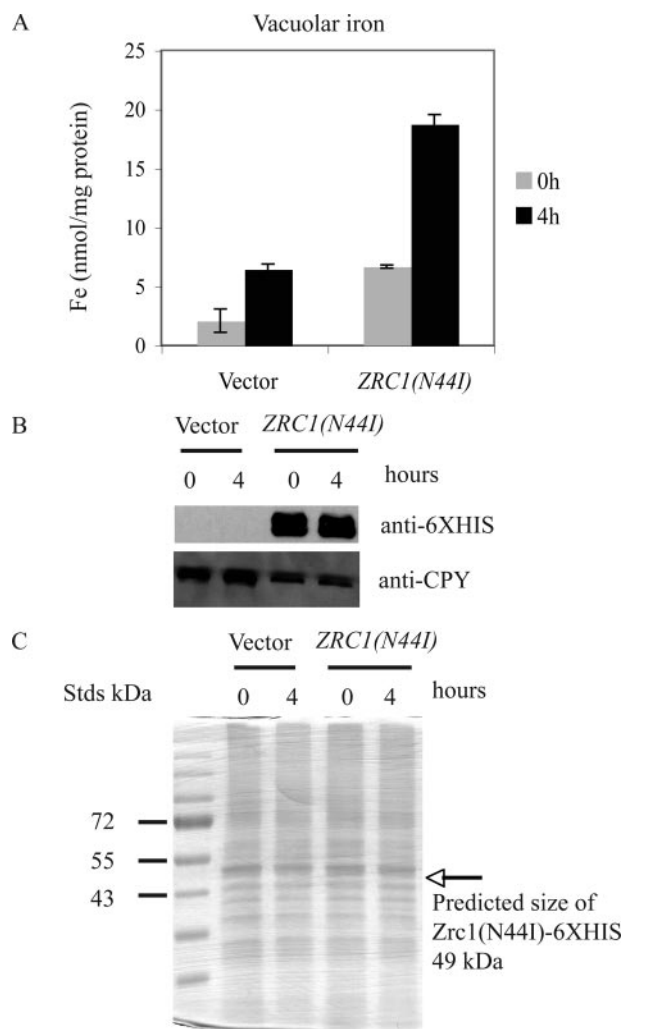
band corresponding to Zrc1(N44I)-HIS$_6$ was not notable (Fig. 6*C*), suggesting that the protein abundance would be insufficient to bind vacuolar iron.

Zrc1(N44I) Transports Manganese—Many transporters that transport iron also transport Mn^{2+} (25, 26). Deletion of *CCC1* results in sensitivity to high Mn^{2+} (27), although with the concentrations and strain used here the sensitivity was slight at best. Expression of *ZRC1(N44I)* suppressed Mn^{2+} toxicity in Δ*ccc1* cells to a greater extent than *ZRC1* (Fig. 7*A*). Pmr1 is a Golgi membrane P-type ATPase involved in transporting Ca^{2+} and Mn^{2+} into the Golgi (28). Deletion of *PMR1* leads to accumulation of Mn^{2+} in the cytosol, increasing the sensitivity of cells to high concentrations of Mn^{2+}. Indeed, *CCC1* was identified as a high copy suppressor of Δ*pmr1* Mn^{2+} toxicity phenotype, indicating it also transports Mn^{2+} into vacuoles (27).

Overexpression of *CCC1* or *ZRC1*(*N44I*), but not wild type *ZRC1*, protected Δ*pmr1* cells from Mn^{2+} toxicity (Fig. 7*B*). These results indicate that Zrc(N44I) also has the ability to transport Mn^{2+}. To examine whether *ZRC1*(*N44I*) can transport copper into vacuoles, we studied the effect of overexpression of *ZRC1*(*N44I*) in copper-sensitive cells. *ACE1* encodes a transcription factor that regulates the expression of metallothioneins, small intracellular proteins that can bind and detoxify copper (29). Deletion of *ACE1* renders cells copper sensitive but overexpression of *ZRC1* or *ZRC1*(*N44I*) did not suppress or enhance the copper sensitivity of Δ*ace1* cells (Fig. 7*C*).

FIGURE 7. ***ZRC1*(*N44I*) shows an altered metal specificity.** *A*, wild type (*WT*) cells (DY150) transformed with empty vector or Δ*ccc1* cells transformed with empty vector, *ZRC1*, or *ZRC1*(*N44I*) were spotted onto CM-Ura plates, CM-Ura plates with 15 mM $MnCl_2$. Plates were incubated at 30 °C for 3 days. *B*, wild type cells (BY4743) or Δ*pmr1* cells were transformed with empty vector, *CCC1*, *ZRC1*, or *ZRC1*(*N44I*) in a high copy vector with their native promoter. Cells were spotted onto CM-Leu plates with or without 2 mM $MnCl_2$. Plates were incubated at 30 °C for 2 days. *C*, wild type cells (BY4743) or Δ*ace1* cells were transformed with empty vector, *CCC1*, *ZRC1*, or *ZRC1*(*N44I*) in a high copy vector with their native promoter. Cells were spotted onto CM-Leu plates with or without 250 μM $CuSO_4$. Plates were incubated at 30 °C for 2 days.

Cot1(N45I) Shows Increased Iron Transport and Decreased Cobalt Transport—The N44I mutation in Zrc1 is in the second hydrophobic domain. The sequence of this domain is highly conserved in homologous CDF proteins involved in Zn^{2+} transport, which are found throughout the biological kingdoms (Fig. 8). This sequence is highly conserved in the Zrc1 homologue Cot1, which shows 78% amino acids similarity to Zrc1. Cot1 was initially identified as a gene that conferred cobalt resistance when overexpressed (4). Cot1 has Zn^{2+} transport activity, as overexpression of *COT1* confers zinc resistance and deletion of *COT1* increases zinc sensitivity in Δ*zrc1* cells (30). The corresponding asparagine at position 45 of Cot1 was changed to isoleucine by site-directed mutagenesis to examine the effect on the substrate specificity of Cot1. Wild type *COT1* or *COT1*(*N45I*) were transformed into Δ*ccc1* cells and growth on high iron medium was examined. High copy expression of *COT1* in Δ*ccc1* cells was able to confer high iron resistance (Fig. 9*A*). Expression of *COT1*(*N45I*) increased the resistance of Δ*ccc1* cells to high iron. Overexpressed *COT1*(*N45I*) was able to induce *FET3-lacZ* reporter expression (Fig. 9*B*) and reduce expression of the *CCC1-lacZ* reporter (Fig. 9*C*) indicating an alteration of iron homeostasis. The N45I mutation, however, decreased the ability of *COT1* to confer cobalt resistance on Δ*cot1* cells (Fig. 9*D*).

Overexpression of *COT1* can partially suppress the high iron growth deficit of Δ*ccc1* cells (Fig. 9*A*), suggesting that Cot1 may be a low affinity iron transporter. In CM medium, however, expression of *COT1* has little effect on *Fet3-lacZ* activity. *COT1* is a target of the transcription factors Aft1 and Aft2 (31) and shows a modest induction under low iron conditions. Low iron conditions prevent accumulation of the vacuolar iron transporter Ccc1, as *CCC1* transcription is activated under high iron conditions (15) and *CCC1* mRNA is destabilized under low iron conditions by the Aft1-regulated gene *CTH2* (14). We considered the possibility that expression of a low affinity vacuolar iron transporter might protect cells against iron shock. Compelling evidence shows that expression of Zrc1 by low zinc conditions protects cells against sudden increases in cytosolic zinc, termed zinc shock (7). We tested the possibility that Cot1 might play an analogous role and protect cells from "iron shock." Cells grown in low iron were transferred to high iron medium and growth assayed. Wild type cells showed no obvious growth defect when incubated in high iron (Fig. 10). In contrast, Δ*ccc1* cells showed a severe growth deficiency. Deletion of *COT1* by itself did not affect growth in high iron nor did it exacerbate the growth defect of a *CCC1* deletion. These results do not support a role for Cot1 in either iron shock conditions or in protecting cells from high iron.

DISCUSSION

Deletion of the vacuolar iron transporter Ccc1 results in growth inhibition on high iron medium. We initiated this study to identify genes that suppressed the high iron growth defect. Our study identified both recessive and dominant muta-
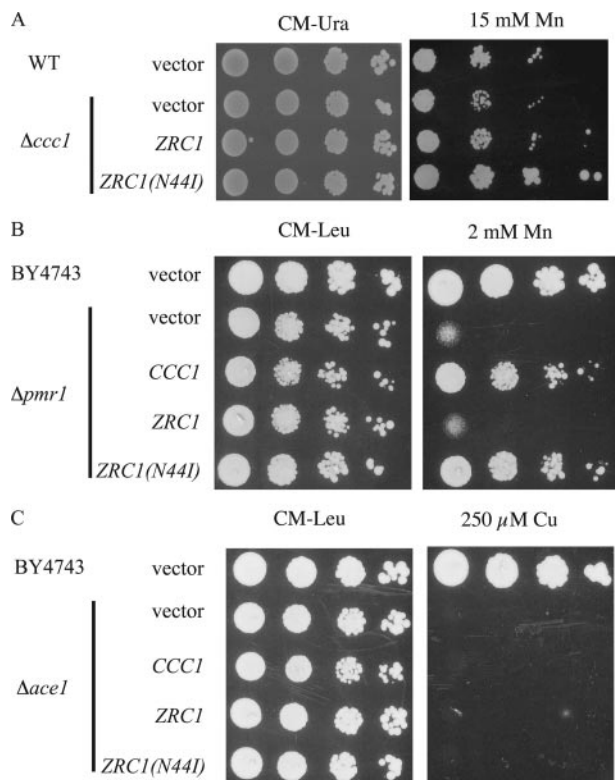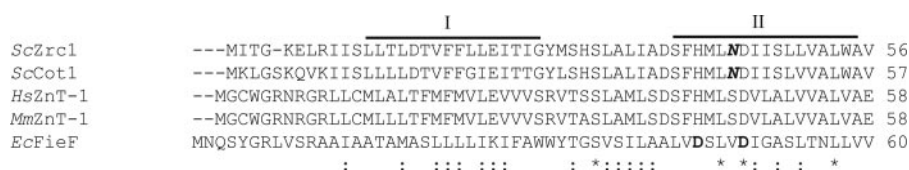

FIGURE 8. **Alignment of Zrc1 homologues.** The Zrc1 protein sequence was used to BLAST search its homologues in other species. Sequences of selected homologues were retrieved and aligned with ClustalW2. *E. coli* FieF, a CDF member, whose structure has already been determined, was also included in the alignment. The position of the mutated amino acids (*N*) in Zrc1 and Cot1 is indicated in *italic*. The two aspartate residues involved in zinc binding in *E. coli* FieF are *bolded*. The predicated transmembrane domains are indicated. The abbreviations are: *Sc, S. cerevisiae*; *Hs, Homo sapiens*; *Mm, Mus musculus*; *Ec, E. coli* K-12. *Asterisk* (*) denotes identity; *colon* (:) denotes similarity.
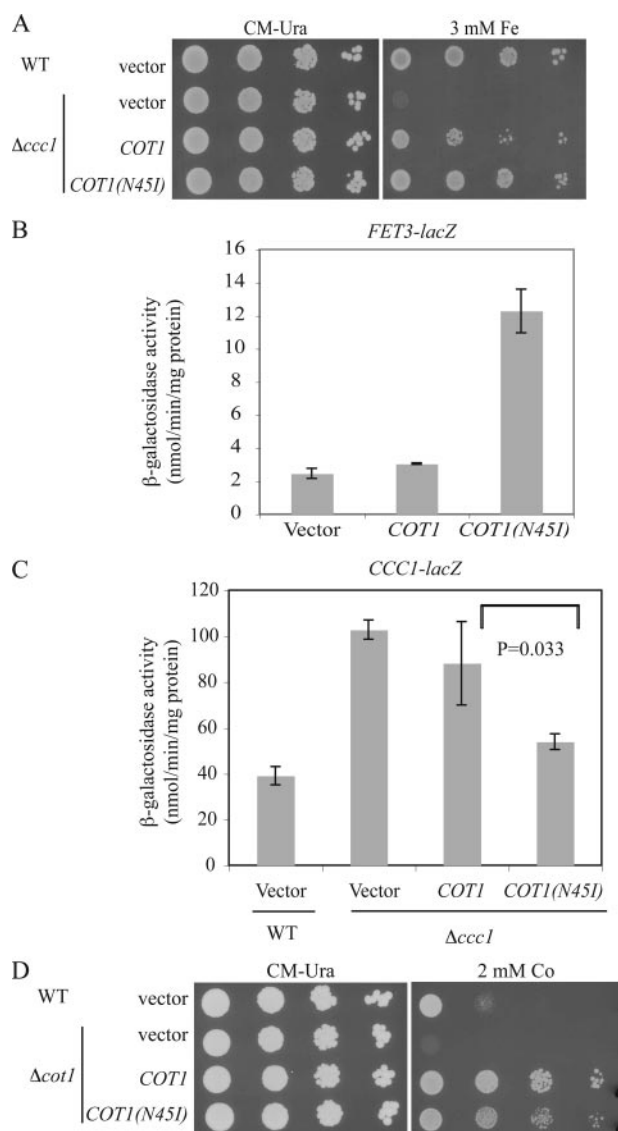
FIGURE 9. **COT1(N45I) protects Δ*ccc1* cells from high iron toxicity.** *A*, wild type (*WT*) cells transformed with a high copy empty vector and Δ*ccc1* cells transformed with empty vector, *COT1*, or *COT1(N45I)* under the *COT1* promoter were spotted onto CM-Ura plates with or without 3 mM ferrous ammonium sulfate. Plates were incubated at 30 °C for 2 days. *B*, WT cells containing an integrated *FET3-lacZ* at the *HO* locus were transformed with a high copy empty vector, *COT1*, or *COT1(N45I)* under the *COT1* promoter. Cells were grown to log phase and β-galactosidase activity determined. *C*, WT cells transformed with a high copy empty vector, Δ*ccc1* cells transformed with empty vector, *COT1*, or *COT1(N45I)* were transformed with a *CCC1-lacZ* reporter construct. Cells were grown to log phase and β-galactosidase activity determined. The data are normalized for protein concentrations and *error bars* represent S.D. from three experiments. *D*, wild type cells (BY4743) transformed with a high copy empty vector and Δ*cot1* cells transformed with empty vector, *COT1*, or *COT1(N45I)* under the *COT1* promoter were spotted onto CM-Ura with or without 2 mM CoCl₂. Plates were incubated at 30 °C for 2 days.

tions that permitted Δ*ccc1* cells to grow on high iron medium. The recessive genes fell into two complementation groups. We also identified eight dominant mutants, which were due to mutations in single genes, although genetic analysis did not permit us to determine whether the dominant mutants were in the same or different genes. Phenotypic analysis suggested that the dominant genes show differences in iron sensitivity and in their ability to modulate cytosolic iron levels (Figs. 1 and 2).
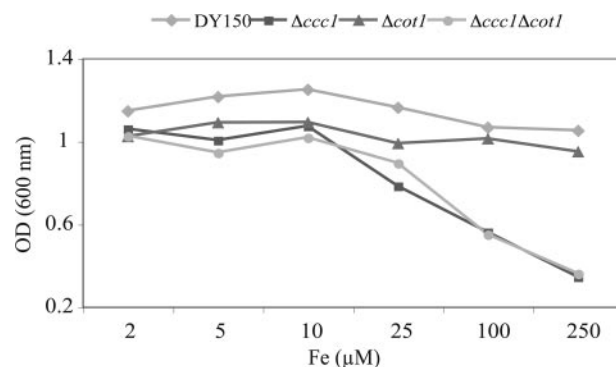

FIGURE 10. **COT1 is not involved in iron shock.** WT cells, Δ*ccc1*, Δ*cot1*, and Δ*ccc1*Δ*cot1* were grown in CM medium with 40 μM BPS overnight. Cells were washed and inoculated into CM medium with 40 μM BPS and specified concentrations of FeSO₄. Cell density was determined 12 h later. The experiment was performed multiple times and a representative experiment is presented.

Only one of the mutants showed notable resistance to oxidants suggesting that modulation of iron-dependent oxygen toxicity is not a prominent mechanism for high iron resistance. This result confirms our previous observation that high iron toxicity does not necessarily result from increased Fenton chemistry, as high iron growth deficit occurs anaerobically.

We identified the molecular basis of one of the dominant iron-resistant mutants to be a single amino acid mutation in the vacuolar Zn^{2+} transporter Zrc1 (22, 30). Targeted site-specific mutagenesis is the most common approach to examining the substrate specificity of enzymes or transporters. In combination with either structural studies or genome wide informatics, targeted mutations have revealed much about the importance of specific domains or amino acids in determining substrate specificity. The role of amino acids in determining the substrate selectivity or transporters has been reported previously for such transporters, as the plant potassium transporter HKT1 (32), H^+-sucrose symporter AtSUC1 from *Arabidopsis thaliana* (33), plasma membrane H^+-ATPase PMA2 from *Nicotiana plumbaginifolia* (34), the plant *A. thaliana* ZIP family member metal transporter IRT1 (35), and yeast *Saccharomyces cerevisiae* Mn^{2+}/Ca^{2+} transporter Pmr1 (36). Amino acid substitutions generally abolish transporter activity or increase the transport activity of one of its substrates relative to another. Here we show that a single amino acid substitution in Zrc1 or Cot1 dramatically changed the substrate specificity. Genetic and biochemical studies have shown that Zrc1 is able to transport Zn^{2+}, Ni^{2+}, Cd^{2+}, but not Fe^{2+} or Mn^{2+} (9). We confirmed this conclusion by measuring resistance to high iron growth conditions and by reporter constructs that assay cytosolic iron levels. Substitution of an asparagine at position 44 to an isoleucine abolished the ability of Zrc1 to transport Zn^{2+} but conferred the ability to transport Fe^{2+} and Mn^{2+}. A similar change in Cot1 also altered its substrate specificity to iron while reducing its ability to transport Co^{2+}.

Zrc1 and Cot1 belong to the CDF family of transition metal transporters. Members of this family are found in all biological kingdoms and most usually transport metals out of the cytosol either into organelles or out of cells. CDF transporters usually have six transmembrane regions in which there is a high degree of sequence conservation in the charged residues of transmem-

brane domains II and V, which is thought to bind metals and form a transmembrane pore. The structure of the *E. coli* CDF member FieF, which transports iron, has been determined with Zn^{2+} in the metal binding site (23). Structural and mutagenesis studies using *E. coli* FieF have focused on the importance of the Asp[45] and Asp[49] in transmembrane TMD II, and His[153] and Asp[157] in TMD V as residues that coordinate Zn^{2+} in the crystal structure, and by implication iron in the native transporter. These charged residues are conserved in CDF family members although each family member shows different substrate specificities. The mutated asparagine is adjacent to the conserved aspartic acid in TMD II of Zrc1 and Cot1. The substitution of a hydrophilic residue with a hydrophobic residue may alter the conformation of the metal binding site, changing the metal specificity of transport. Our study suggests that the microenviroment of the amino acids adjacent to the metal binding aspartate determines the substrate selectivity. The mutated *ZRC1* was identified by a screen using random UV mutagenesis to select for cells showing high iron resistance. The approach of using a strong selection system in conjunction with mutagenesis of genes encoding transporters offers the possibility of facile identification of other residues critical for determining the substrate specificity of CDF transporters.

REFERENCES

1. Ramsay, L. M., and Gadd, G. M. (1997) *FEMS Microbiol. Lett.* **152,** 293–298
2. Eide, D. J., Bridgham, J. T., Zhao, Z., and Mattoon, J. R. (1993) *Mol. Gen. Genet.* **241,** 447–456
3. Szczypka, M. S., Zhu, Z., Silar, P., and Thiele, D. J. (1997) *Yeast* **13,** 1423–1435
4. Conklin, D. S., McMaster, J. A., Culbertson, M. R., and Kung, C. (1992) *Mol. Cell. Biol.* **12,** 3678–3688
5. Kamizono, A., Nishizawa, M., Teranishi, Y., Murata, K., and Kimura, A. (1989) *Mol. Gen. Genet.* **219,** 161–167
6. Li, L., Chen, O. S., McVey Ward, D., and Kaplan, J. (2001) *J. Biol. Chem.* **276,** 29515–29519
7. MacDiarmid, C. W., Milanick, M. A., and Eide, D. J. (2003) *J. Biol. Chem.* **278,** 15065–15072
8. Simm, C., Lahner, B., Salt, D., LeFurgey, A., Ingram, P., Yandell, B., and Eide, D. J. (2007) *Eukaryot. Cell* **6,** 1166–1177
9. MacDiarmid, C. W., Milanick, M. A., and Eide, D. J. (2002) *J. Biol. Chem.* **277,** 39187–39194
10. Montanini, B., Blaudez, D., Jeandroz, S., Sanders, D., and Chalot, M. (2007) *BMC Genomics* **8,** 107
11. Wei, Y., Li, H., and Fu, D. (2004) *J. Biol. Chem.* **279,** 39251–39259
12. Grass, G., Otto, M., Fricke, B., Haney, C. J., Rensing, C., Nies, D. H., and Munkelt, D. (2005) *Arch. Microbiol.* **183,** 9–18
13. Kim, S. A., Punshon, T., Lanzirotti, A., Li, L., Alonso, J. M., Ecker, J. R., Kaplan, J., and Guerinot, M. L. (2006) *Science* **314,** 1295–1298
14. Puig, S., Askeland, E., and Thiele, D. J. (2005) *Cell* **120,** 99–110
15. Li, L., Bagley, D., Ward, D. M., and Kaplan, J. (2008) *Mol. Cell. Biol.* **28,** 1326–1337
16. Li, L., and Kaplan, J. (2004) *J. Biol. Chem.* **279,** 33653–33661
17. Amberg, D. C., Botstein, D., and Beasley, E. M. (1995) *Yeast* **11,** 1275–1280
18. Crisp, R. J., Pollington, A., Galea, C., Jaron, S., Yamaguchi-Iwai, Y., and Kaplan, J. (2003) *J. Biol. Chem.* **278,** 45499–45506
19. Ausubel, F. M. (1995) *Current Protocols in Molecular Biology*, Wiley, New York
20. Calvin, N. M., and Hanawalt, P. C. (1988) *J. Bacteriol.* **170,** 2796–2801
21. Tuttle, M. S., Radisky, D., Li, L., and Kaplan, J. (2003) *J. Biol. Chem.* **278,** 1273–1280
22. MacDiarmid, C. W., Gaither, L. A., and Eide, D. (2000) *EMBO J.* **19,** 2845–2855
23. Lu, M., and Fu, D. (2007) *Science* **317,** 1746–1748
24. Yamaguchi-Iwai, Y., Dancis, A., and Klausner, R. D. (1995) *EMBO J.* **14,** 1231–1239
25. Dix, D. R., Bridgham, J. T., Broderius, M. A., Byersdorfer, C. A., and Eide, D. J. (1994) *J. Biol. Chem.* **269,** 26092–26099
26. Forbes, J. R., and Gros, P. (2003) *Blood* **102,** 1884–1892
27. Lapinskas, P. J., Lin, S. J., and Culotta, V. C. (1996) *Mol. Microbiol.* **21,** 519–528
28. Lapinskas, P. J., Cunningham, K. W., Liu, X. F., Fink, G. R., and Culotta, V. C. (1995) *Mol. Cell. Biol.* **15,** 1382–1388
29. Winge, D. R. (1998) *Prog. Nucleic Acids Res. Mol. Biol.* **58,** 165–195
30. Conklin, D. S., Culbertson, M. R., and Kung, C. (1994) *Mol. Gen. Genet.* **244,** 303–311
31. Rutherford, J. C., Jaron, S., and Winge, D. R. (2003) *J. Biol. Chem.* **278,** 27636–27643
32. Rubio, F., Gassmann, W., and Schroeder, J. I. (1995) *Science* **270,** 1660–1663
33. Lu, J. M., and Bush, D. R. (1998) *Proc. Natl. Acad. Sci. U. S. A* **95,** 9025–9030
34. Morsomme, P., de Kerchove d'Exaerde, A., De Meester, S., Thines, D., Goffeau, A., and Boutry, M. (1996) *EMBO J.* **15,** 5513–5526
35. Rogers, E. E., Eide, D. J., and Guerinot, M. L. (2000) *Proc. Natl. Acad. Sci. U. S. A* **97,** 12356–12360
36. Mandal, D., Woolf, T. B., and Rao, R. (2000) *J. Biol. Chem.* **275,** 23933–23938